Experimental Study on Seismic Retrofit by Using Supplemental Knee Braces Attached to Steel Members with Semi-Rigid Bolted Connections

Y. Harada
Chiba University, Chiba, Japan

K. Ebato & S. Honma
Kanto Gakuin University, Yokohama, Japan

T. Takimoto
Tokyo-Kenchiku structural engineers, Tokyo, Japan

SUMMARY:
Attachment of supplemental knee braces to existing steel frameworks is one of the most efficient seismic retrofitting measures. Existing steel members should be properly reinforced at the sections where the knee braces are to be attached in order to prevent local deformation of the existing members. In some buildings, on-site welding is restricted, and then the local reinforcement must depend only on bolted connections of the steel member to the knee brace. In such cases, the connections would be not rigid, but semi-rigid. The purpose of this study is to demonstrate experimentally that supplemental knee braces work well as seismic upgrading members, even if they are attached semi-rigidly. The discussion is based on the results of cyclic loading tests with beam-to-column subassemblage specimens and corresponding finite element analysis (FEA). A macro-model with local deformation spring components for the knee-braced framework is also proposed on the basis of the discussion.

Keywords: Steel building structure, knee brace, bolted connection, semi-rigid connection, component model

1. INTRODUCTION

Attachment of supplemental knee braces to steel members in existing steel structures is regarded as one of the most efficient seismic retrofitting measures. Existing steel members (i.e., beams and columns) should be properly reinforced at sections where the knee braces are to be attached; otherwise, the plate elements of the existing member might deform locally under seismic excitation, and the axial stiffness of the knee brace would then be reduced owing to local deformation.

Such a local reinforcement is generally achieved by welding stiffening plates to the existing members. However, on-site field welding is restricted in some buildings due to the risk of fire caused by welding arcs, so local reinforcement should be achieved only using bolted connections and reinforcing joint metals. In such cases, the connections between the knee braces and the existing members cannot be rigid; therefore, they should be designed as semi-rigid due to the local deformation of the existing members.

The purpose of the present study is to demonstrate experimentally that supplemental knee braces work well as seismic-retrofitting members, even if they are attached semi-rigidly to the existing members with only high-strength bolted connections. These discussions are about plane steel frameworks with wide flange (H-section) weak-axis columns and wide flange beams. In this type of older existing steel framework, poor lateral stiffness and strength are often problems.

2. CYCLIC LOADING TESTS OF BEAM-TO-COLUMN SUBASSEMBLAGE SPECIMENS

To verify the efficiency of supplemental knee braces, a series of cyclic loading tests of subassemblage specimens were conducted. For two types of subassemblages, unreinforced (i.e., without knee braces) and reinforced (i.e., with knee braces) T-shaped and cruciform specimens were prepared (Fig. 2.1). The beam-to-column-web connections were non-weld double split-T type semi-rigid connections (Harada et al. 2008). Although this type of beam-to-column connection is uncommon, the effectiveness of knee bracing on frameworks with the ordinary welded connections could be safely estimated from the results with the double split-T connections, because the connection rigidity of this type is lower than that of ordinary welded connections due to local deformation of the unstiffened column web plates. It should be noted that this situation is the same as that for the knee brace reinforcement of steel frameworks with hollow section columns (Takagi et al. 2003). The experimental results from the subassemblage cyclic loading tests are summarized here, and the details of the experimental results are presented in the authors' previous studies (Ebato et al. 2005, Nomote et al. 2009, Honma et al. 2012).

2.1 Outline of cyclic loading tests of subassemblages

The subassemblage specimens consisted of wide flange beams and columns, which were connected using split-tee stubs and high-strength bolts, without welding (Fig. 2.1(a), (b)). The reinforcing knee brace member was also attached to the beam and the column using split-tee stubs and high-strength bolts. The knee brace is a double channel section, and the channels and the split-tees were also connected using high-strength bolts (Fig. 2.1(c)). The knee brace was inclined to the beam member at an angle of 45°. The mechanical properties of the column, beam, split-tee, and channel are listed in Table 2.1. The top and bottom of the column were supported by pin or roller supports. Static cyclic reversal loading was applied to the beam end by hydraulic actuators (Fig. 2.1(d)). The loading is displacement-controlled for lateral drift angle (R); the target drift amplitudes were 0.005, 0.01, 0.02, 0.04, and 0.06 rad.

2.2 Experimental Overall Deformation Behavior

Fig. 2.2 shows the experimental column shear force (Q_c)−drift angle (R) relationship curves; the column shear force Q_c was calculated from the beam-end load Q_b by simple statics as the reaction force at the column supports. The figures indicated that the initial stiffness and general yield strength of the unreinforced subassemblages were enhanced by approximately a factor of two to three by reinforcing with the knee brace. Every specimen exhibited a stable spindle shape until a drift angle of 0.02 rad, although under larger drift cycles, hysteretic loops began to show pinching. These stable and spindle-shaped hysteretic loops indicated good deformation capacity of the frameworks.

It should be noted that the critical portions for overall yielding changed if a reinforcing knee brace was attached. The out-of-plane deformation of the column web was critical for the unreinforced specimens, while flexural yielding of the beam or the column member was critical for the reinforced specimens. The agreement between the experimental yield strengths and the estimated strengths by local yielding (dashed lines shown in the figures) (Ebato et al. 2005, Nomote et al. 2009) also supports the change in the critical portion. From the Q_c−R curves of the unreinforced subassemblages, it can be seen that post-yield tangent stiffness under large deformation was kept almost constant (except the final loop of the cruciform specimen where punching shear failure occurs in the column web plate at the corners of the split-tee flange). This was due to membrane action of the column web with out-of-plane deformation and is specific to this type of connection (Neves et al. 1996).

Table 2.1 Example of material properties (T-shaped reinforced specimen)

	Steel material	Yield stress (N/mm^2)	Tensile stress (N/mm^2)	Yield ratio (%)	Elongation (%)
Column	SN400B	327.0	440.8	74.2	26.3
Beam	SN490B	399.5	561.5	71.1	23.1
Split-tee	SN490B	417.7	568.3	73.5	23.1
Knee brace	SS400	401.0	513.2	78.1	26.6
High strength bolts	S10T-M24	1021.0	1064.7	95.9	-

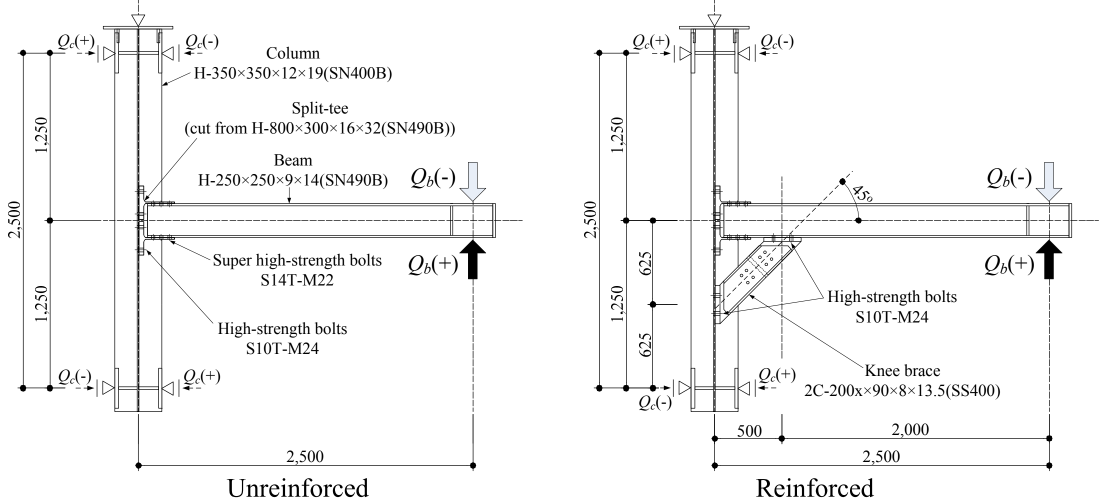

(a) T-shaped subassemblages

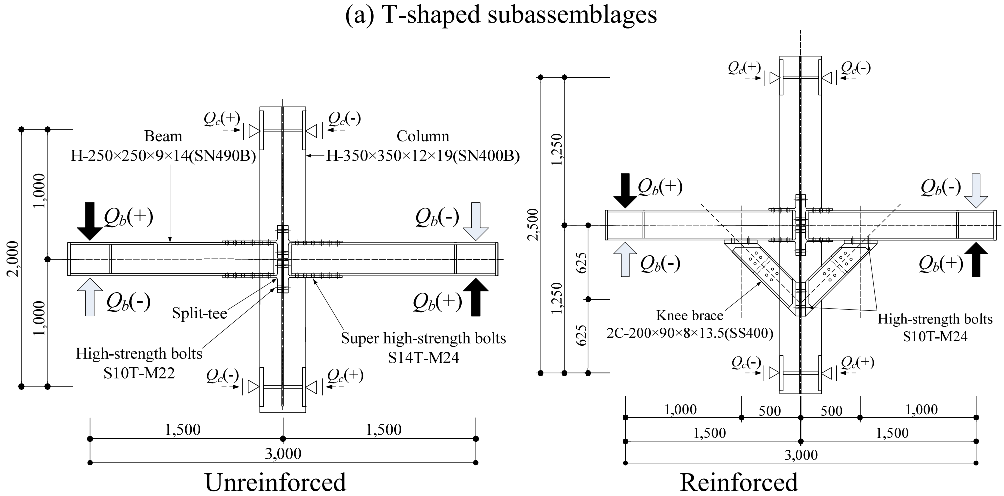

(b) Cruciform subassemblages

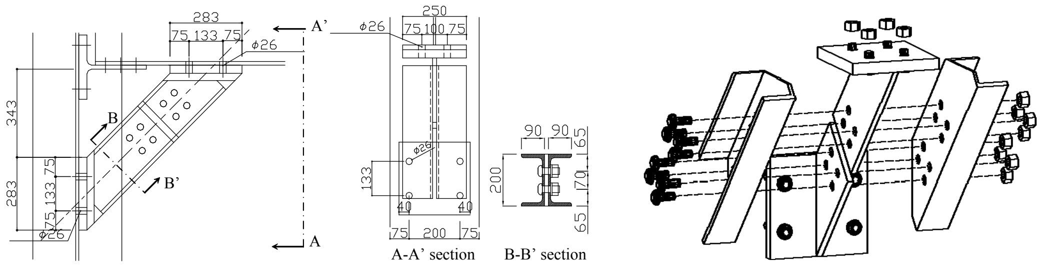

(c) Composition of knee brace member

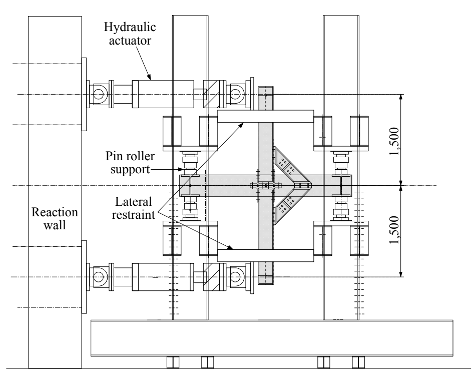

(d) Example of test setup (cruciform subassemblage)

Figure 2.1 Subassemblage specimens

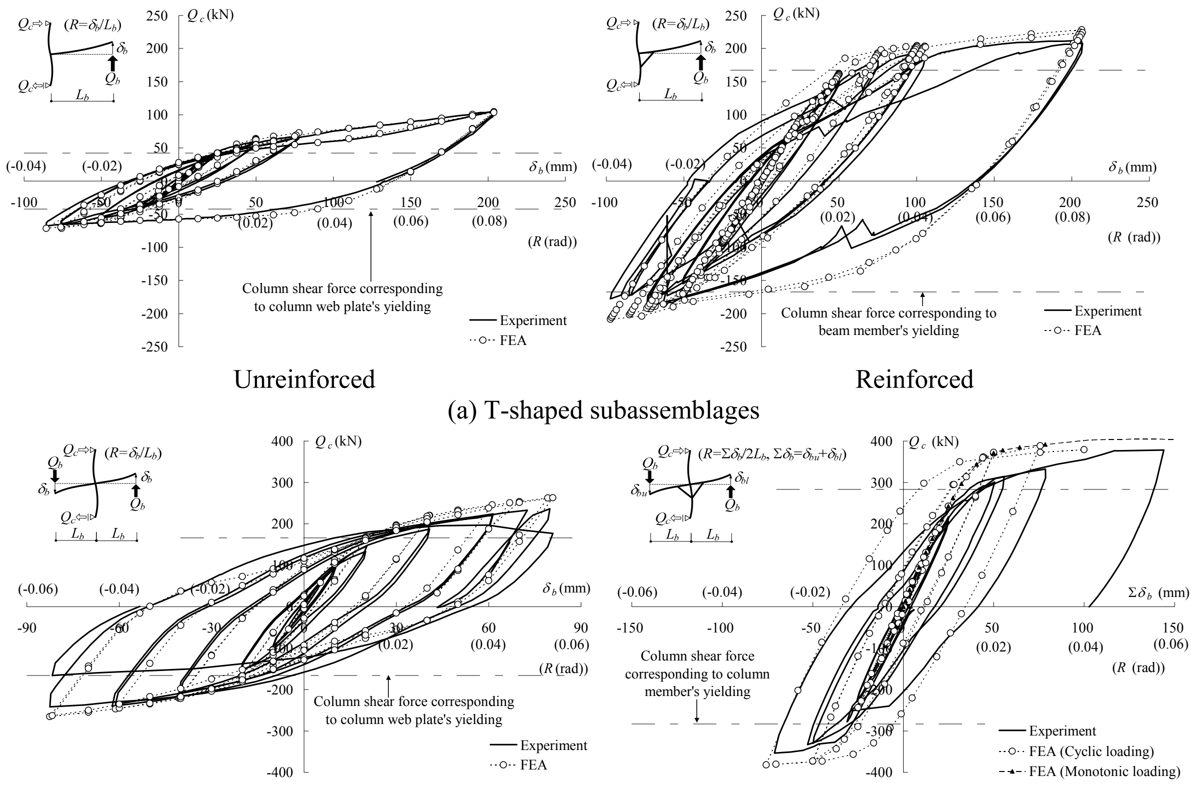

Unreinforced Reinforced

(a) T-shaped subassemblages

Unreinforced Reinforced

(b) Cruciform subassemblages

Figure 2.2 Column shear force (Q_c)-drift angle (R) relationship curves (with FEA results)

3. FINITE ELEMENT ANALYSES OF KNEE-BRACED SUBASSEMBLAGES

To investigate the local deformation behaviors of plate elements near the bolted joints, finite element analysis (FEA) was used in addition to the loading tests described in the previous section. It is shown here that the structural behavior of the knee-braced subassemblage can be simulated by FEA, and the FEA results were verified experimentally.

3.1 Outline of Finite Element Analyses

The FEA was performed using the general-purpose FEA software ANSYS 14.0 (ANSYS, Inc. 2011). Figure 3.1 shows the finite element models for the subassemblage specimens. As the specimen was symmetrical, only one-half of the specimen was modeled. The finite element model was composed of solid eight-node brick elements. High-strength bolts were also modeled by solid elements. Contact between plates and bolts and the tightening of the bolts were modeled in ANSYS by contact and pretension elements, respectively. The stress-strain relationship of the steel material was input by transforming the experimental relationship obtained from coupon tests to true stress-true strain relationship and approximating it to a multi-linear curve. A kinematic hardening plastic model was adopted to consider the cyclic plasticity of the steel material.

3.2 Comparison between Experimental and Simulated Behavior

3.2.1 Overall Behavior

Simulated cyclic behaviors of the subassemblages by FEA are also shown in Fig. 2.2 by dashed lines. The analyses were performed in displacement-controlled for the drift angle R, and the displacement amplitude history was the same as that of the loading tests. The Q_c−R curves in Fig 2.2 show good agreement between the experimental and the simulated results, except for the knee-braced cruciform specimen, which shows larger simulated strength than that measured by experiment under large deformation. The difference in strength means that the beginning of local buckling of the column flange, which is accompanied by weak-axis column member's yielding, could not be captured by FEA.

3.2.2 Local Behavior

Fig. 3.2 shows an example of axial force (N_k) acting on the knee brace and the beam-end load (Q_b) relationship curve for the T-shaped subassemblage. The experimental axial force was calculated from the measured strain by strain gauges attached to the knee brace member. This figure shows that the FEA results show very good agreement with the experimental results. The N_k–Q_b hysteresis curve can be approximated by a single straight line passing through the origin; this indicated that the knee brace member remained elastic.

Fig. 3.3 shows an example of a comparison between FEA and experimental results of out-of-plane deformation of a column web plate. The relationship between the column shear force Q_c and the out-of-plane deformation of the column web at the upper and lower beam flange (${}_u\delta_L$ and ${}_u\delta_L$, respectively, Fig. 3.3(a)) and that at the knee-brace-end (${}_k\delta_L$, Fig. 3.3(b)) are shown. The experimental out-of-plane deformations were obtained by displacement transducers attached to the specimen. In this figure, the out-of-plane deformations by FEA underestimate the experimental ones under larger Q_c. In Fig. 3.3(a), a large deformation can be observed at the upper split tee, although little deformation is observed at the lower split tee. This implies that only slight out-of-plane tensile force works on the column web plate at the lower split tee, and thus, the beam-end bending moment is mainly transferred to the column member as a force couple consisting of forces in the out-of-plane direction at the upper split tee and that at the knee-brace joint. The validity of the above implication for a resisting mechanism in the beam-end and knee-brace-end connections will be discussed in the next section.

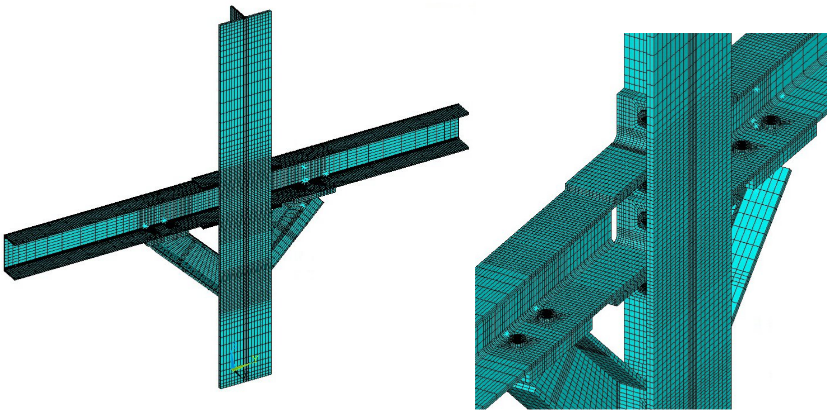

Figure 3.1 Example of finite element model (Cruciform reinforced specimen)

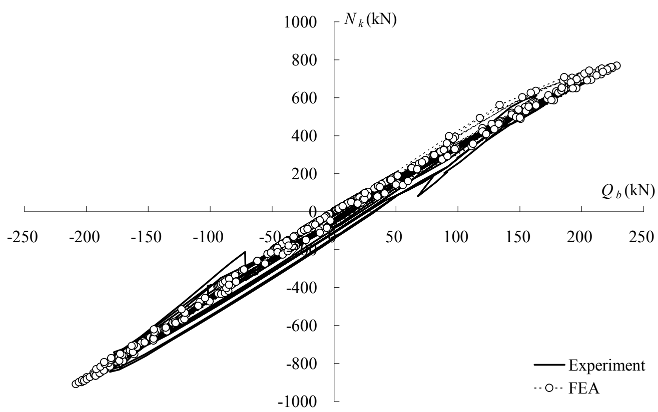

Figure 3.2 Comparison of axial force of knee brace member (T-shaped reinforced specimen)

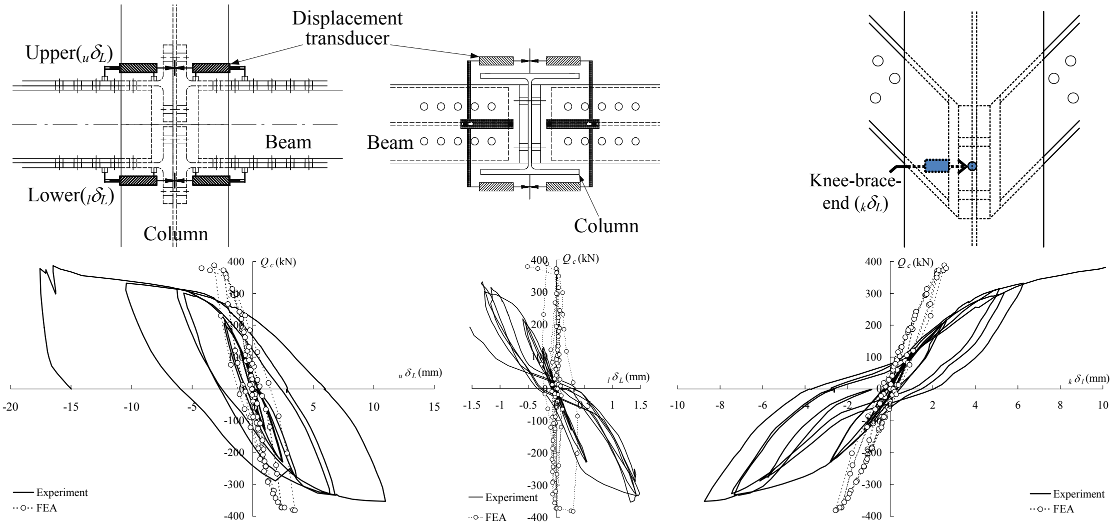

(a)Beam-end-to-column web connection (b)Knee-brace-end-to-column web connection

Figure 3.3 Comparison of out-of-plane deformation of column web plate (cruciform reinforced specimen)

4. MACRO-MODEL FOR SEMI-RIGIDLY KNEE-BRACED FRAMEWORK

4.1 Macro-Model to Predict Overall Behavior of Knee-Braced Framework

In the previous section, it was shown that the structural behavior of knee-braced steel frameworks can be accurately estimated by FEA. However, for practical structural design, a much simpler analysis method should be developed. A macro-model for estimating structural behavior of knee-braced steel frameworks with semi-rigid connections is proposed here (Fig. 4.1). The proposed macro-model is based on the concept of the component model in Eurocode 3. A split-tee-column web plate connection was modeled by a single tension-only spring component, which represented the out-of-plane deformation of the column web plate. This spring component deformed only under tensile force, because the compressive force on the spring component was transferred by the surface contact between the split-tee flange and the column web, and thus, the deformation due to compressive force was very much smaller than that due to tensile force.

For the connection design in the vicinity of the knee brace member, the tensile forces acting on the spring components should be estimated. They correspond to the reaction forces at the column web, i.e., $_jP_u$ at the upper flange of the beam, $_jP_l$ at the lower flange of the beam, and $_jP_k$ at the knee-brace-end. The predictive model for the tensile force in the spring components is presented here. To accomplish that, the beam and the knee brace member are assumed to be rigid (Fig. 4.1).

It should be noted that the resisting mechanism of the knee-braced framework depends on whether the knee brace is in tension or in compression, because the local out-of-plane spring deforms by tension only. If the knee brace is in tension (Fig. 4.2), the upper beam flange spring is in compression without deformation, and the lower beam flange spring and the knee-brace-end spring are in tension and deformed outward. In contrast, if the knee brace is in compression (Fig. 4.3), the knee-brace-end spring is in compression without deformation, and the upper and lower beam-end spring components are in tension and deformed outward; the beam-end spring components are pulled by the tensile force acting at on the beam-end, which corresponds to the compression of the knee-brace member.

4.1.1 When the knee brace is in tension

Fig. 4.2 shows the modeled behavior where the knee brace is in tension (Fig 4.2(a)); the sign of the reaction force $_jP$ is assumed to be positive when the spring component is in tension. From equilibrium of lateral force and moment, the following relationships are obtained:

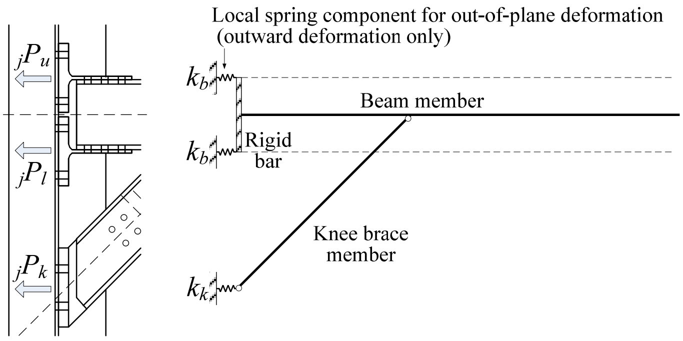

Figure 4.1 Local out-of-plane spring components at the beam-end and the knee-brace-end

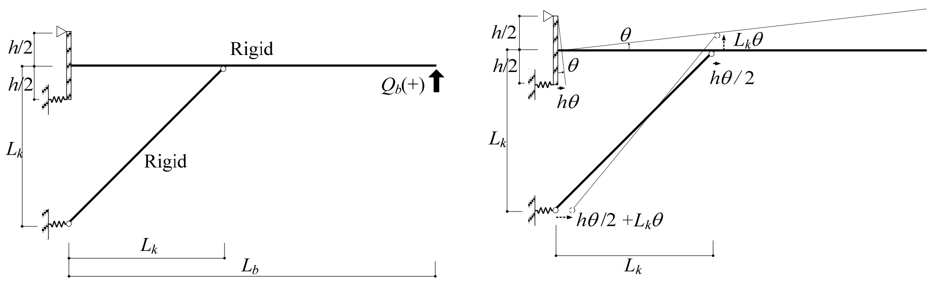

(a) Assumed configuration (b) Overall deformation

Figure 4.2 Macro-models for vicinity of beam-column joint and knee brace (the knee brace in tension)

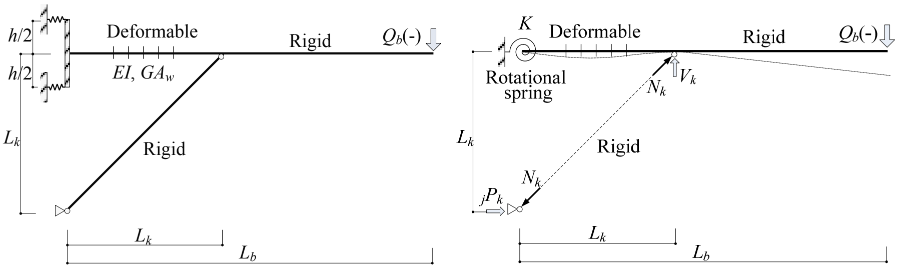

(a) Assumed configuration (b) Overall deformation

Figure 4.3 Macro-models for vicinity of beam-column joint and knee brace (the knee brace in compression)

$$_jP_u + {_jP_l} + {_jP_k} = 0\,, \tag{1}$$

$$Q_b \cdot L_b + {_jP_u} \cdot (L_k + h/2) + {_jP_l} \cdot (L_k - h/2) = 0\,. \tag{2}$$

From geometrical consideration of the deformations of the local springs at the lower beam flange and at the knee brace (Fig 4.2(b)), the following relationship with spring constants of beam-end k_b and knee-brace-end k_k should hold:

$$\frac{_jP_k}{_jP_l} = \frac{h/2 + L_k}{h} \cdot \frac{k_k}{k_b} \left(\equiv \frac{h/2 + L_k}{h} \cdot k',\ k' \equiv \frac{k_k}{k_b} \right). \tag{3}$$

From Equations (1), (2), and (3), the reaction forces at the column web are obtained as follows:

$$_jP_u = -Q_b \times \{L_b h + L_b (L_k + h/2) \cdot k'\} / \{h^2 + (L_k + h/2)^2 \cdot k'\}, \tag{4-1}$$

$$_jP_l = Q_b \times L_b h / \{h^2 + (L_k + h/2)^2 \cdot k'\}, \tag{4-2}$$

$$_jP_k = Q_b \times L_b (L_k + h/2) \cdot k' / \{h^2 + (L_k + h/2)^2 \cdot k'\}. \tag{4-3}$$

4.1.2 When the knee brace is in compression

Fig. 4.3 shows the modeled behavior where the knee brace is in compression (Fig 4.3(a)). The solution for the model can be attributed to a solution for the cantilever with midspan roller support and a rotational spring at its fixed end if the knee brace member and the knee-brace-end spring act as rigid body (Fig 4.3(b)). It should be noted that the deformation of the beam member between the beam-end and knee-brace-end should be taken into account to solve the problem; the cantilever under such a constraint condition could not deform, if the beam member is rigid. This is in contrast to the case when the knee brace is in tension.

The cantilever can be solved as a statically indeterminate beam with one degree of static indeterminacy. Then, the vertical reaction force at the midspan support V_k is derived as follows:

$$V_k = Q_b \times \frac{\dfrac{L_k}{L_b}\left(3-\dfrac{L_k}{L_b}\right)+\kappa\dfrac{6EI}{GA_wL_b{}^2}+\dfrac{6EI}{KL_b}}{2\left(\dfrac{L_k}{L_b}\right)^2+\kappa\dfrac{6EI}{GA_wL_b{}^2}+\dfrac{L_k}{L_b}\cdot\dfrac{6EI}{KL_b}} \quad (\equiv Q_b \times v). \tag{5}$$

A non-dimensional constant v in this equation is determined by the ratios L_k/L_b (<1) and $\kappa \cdot 6EI/(GA_wL_b{}^2)$. Since the rotational stiffness K ranges from zero to infinity, the range of v is obtained as follows:

$$\frac{\dfrac{L_k}{L_b}\left(3-\dfrac{L_k}{L_b}\right)+\kappa\dfrac{6EI}{GA_wL_b{}^2}}{2\left(\dfrac{L_k}{L_b}\right)^2+\kappa\dfrac{6EI}{GA_wL_b{}^2}} < v < \frac{1}{\dfrac{L_k}{L_b}} \quad \left(\text{if } 1<\kappa\dfrac{6EI}{GA_wL_k{}^2}\right). \tag{6}$$

The inequality condition on the knee-brace length L_k in Equation (6) holds provided that L_k is not too long.

The equilibrium among the compressive axial force of the knee-brace member N_k, the vertical reaction force at the midspan support V_k, and the knee-brace-end reaction ${}_jP_u$ leads to the following relationship:

$${}_jP_k = -V_k = -Q_b \times v\,. \tag{7}$$

The equilibrium of lateral force and moment, given by Equations (1) and (2), respectively, also holds in this case. Then, from (1), (2), and (7), the reaction forces at the column web are obtained as follows:

$${}_jP_u = Q_b \times \left\{\frac{L_b}{h} - v\cdot\left(\frac{L_k}{h}-\frac{1}{2}\right)\right\}, \tag{8-1}$$

$${}_jP_d = Q_b \times \left\{-\frac{L_b}{h} + v\cdot\left(\frac{L_k}{h}+\frac{1}{2}\right)\right\}. \tag{8-2}$$

It should be noted that the rotational stiffness K depends on the condition of the beam-end local springs, i.e., whether the beam-end local springs are in tension or in compression, since the local springs are assumed not to deform under compression.

4.2 Discussions on the Proposed Macro-Model

The validity of the proposed macro-model is discussed here, and the reaction forces at the beam- and the knee-brace-end bolted joints (${}_jP_u$, ${}_jP_l$, ${}_jP_k$) as obtained using the macro-model are compared with those obtained by FEA.

Fig. 4.4(a) shows the reaction forces ${}_jP_u$, ${}_jP_l$, and ${}_jP_k$ for the T-shaped knee-braced specimen as obtained by FEA and using the proposed macro-model. The reaction forces under three loading stages are shown: the corresponding drift angles R are +0.005, +0.01, and +0.04 rad for positive loading (knee brace in tension), −0.005, −0.01, −0.025 rad for negative loading (knee brace in compression). When the knee brace is in tension, the reaction force distribution by FEA is estimated accurately using the macro-model, other than R=+0.04 rad; this is due to stiffness reduction of the spring component by yielding of the column web plate under larger drift. When the knee brace is in compression, the reaction forces at the upper and lower beam flange, ${}_jP_u$ and ${}_jP_l$, respectively, is not estimated accurately. The rotational stiffness K in the macro-model was obtained using the previous experimental results (Nomoto et al. 2008). If K is assumed to be infinity, however, the reaction forces by the macro-model show good agreement with FEA results. This may indicate that the rotational stiffness from the previous experiments was not adequate. This is because the spring component has no definite elastic stiffness since the out-of-plane behavior of the web plate is non-linear even under small deformation. Therefore, the local behaviors of the bolted connections will be able to be roughly estimated by the macro-model, provided that the effective stiffness of the spring component under small out-of-plane deformation is exactly determined.

Fig. 4.4(b) shows the reaction forces ${}_jP_u$, ${}_jP_l$, and ${}_jP_k$ for the cruciform knee braced specimen as obtained by FEA and using the proposed macro-model. The macro-model in the previous section is assumed to be applicable to the cruciform framework by simply combining the T-shaped frameworks with a knee brace in tension and in compression. The reaction forces under the deformation where the drift angle R is 0.005, 0.01, and 0.02 rad are shown. The agreement between the FEA and the macro-model results is almost the same as that for the T-shaped framework.Although the accuracy of the prediction by the macro-model is not very good, the macro-model will be able to be refined. First, rigid body assumptions were made to simplify the macro-model, and then the deformation of every component of the framework can be considered. Second, only single secant stiffness was used as the representative spring constant of the spring component, and then the effective stiffness in accordance with a magnitude of the deformation can be considered.

The yield strengths of the column web plate under local out-of-plane deformation derived by yield line analyses (Ebato et al. 2005, Nomoto et al. 2009) are also shown by dashed lines in Fig. 4.4 (${}_jP_{bp}$ for beam-end connection and ${}_jP_{kp}$ for knee-brace-end connection). It can be observed that the local tensile forces acting on the bolted connections, under the drift angle R smaller than 0.02 rad, are smaller than those yield strengths. This indicates that the knee brace member worked well even when attached with semi-rigid bolted connections.

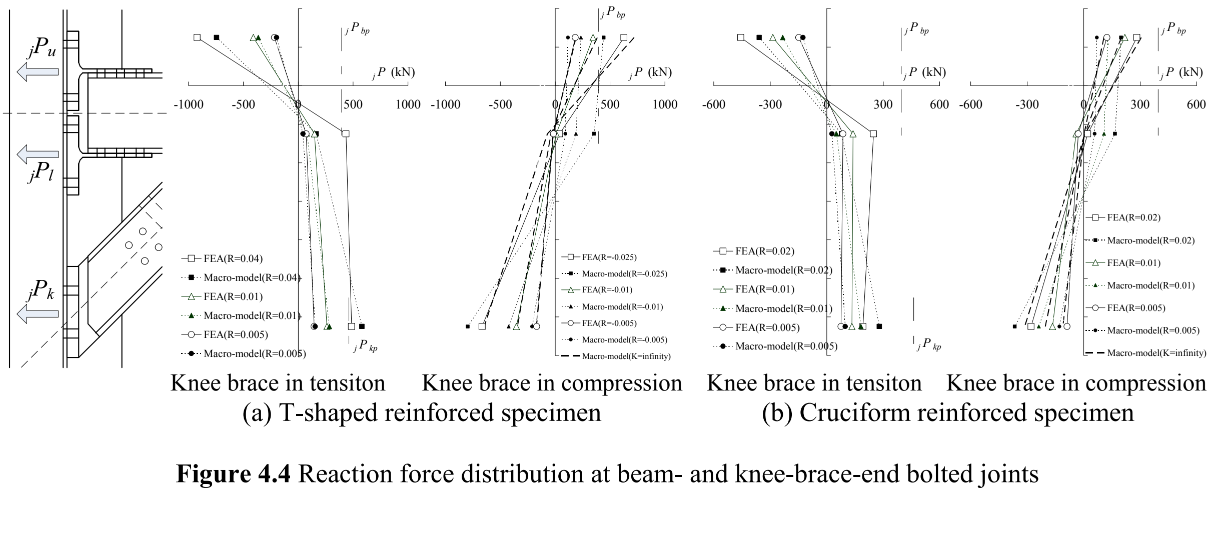

Knee brace in tensiton Knee brace in compression Knee brace in tensiton Knee brace in compression

(a) T-shaped reinforced specimen (b) Cruciform reinforced specimen

Figure 4.4 Reaction force distribution at beam- and knee-brace-end bolted joints

5. CONCLUSION

The effectiveness of supplemental knee brace member was examined by comparing cyclic loading test results for reinforced specimens (i.e., with knee braces) to those of unreinforced specimens (i.e., without the knee braces). The test results indicated that the structural performance of the subassemblage was well enhanced by the supplemental knee braces. The initial stiffness and general yield strength of the unreinforced subassemblage were increased by approximately a factor of two to three, and the cyclic load-deformation relationship curve of the reinforced subassemblage exhibited a stable spindle shape until a large deflection corresponding to a drift angle of 0.02 rad.

Results of corresponding FEA revealed that the experimental structural behaviors of the subassemblages could be simulated accurately. Some experimental observations of local behavior were also seen in the simulated results: the local deformations of the existing beam and column were small, and additional member force acted on the existing member due to attachment of the knee braces.

A macro-model to predict the reaction force at the column plate of the framework reinforced by the supplemental knee brace was proposed on the basis of the experimental and analytical behaviors of the subassemblages. This model consisted of some spring components representing local out-of-plane deformation of the plate elements of the column member. Our intention behind developing this model was to enable the use of a general-purpose frame analysis software to aid in the practical application of supplemental knee bracing. The local tensile force acting on the bolted joints in the beam-end and knee-brace-end connections could be roughly estimated using the proposed macro-model, and the model will be elaborated by removing some simplified assumptions. Results showed that the semi-rigid knee-brace-end connection in the reinforced framework remained elastic under large deflection, and thus, the efficiency of the semi-rigidly attached knee brace was confirmed.

ACKNOWLEDGMENT
This research was supported by JSPS KAKENHI Grant Number 22360221, and 22560575.

REFERENCES

Harada, Y., Ebato, K., and Yagi, J. (2008). Cyclic Behavior of Unstiffened Double Split-Tee Beam-to-Column Connection, *17th Congress of IABSE*, Paper No. A-1064.

Takagi, M., Harada, Y., and Morita, K. (2003) Seismic upgrade of steel framework by supplemental knee-braces. Journal of Constructional Steel. **11**, 415-422. (in Japanese)

Ebato, K., Nomoto, A., Harada, Y., and Morita, K. (2005). Structural Behaviors of H-section Weak Axis Column to H-Section Beam Connection with High Strength Bolts. *Journal of Structural and Construction Engineering (Transactions of AIJ)*. **596**, 109-116. (in Japanese)

Nomoto, A., Ebato, K., and Harada, Y. (2009). Structural behavior of steel framework with knee brace in H-Section weak axis column-to-beam connection with high-strength bolts. *Stessa 2009 (Behaviour of Steel Structures in Seismic Areas)*, 173-179.

Honma, S., Ebato, K., and Harada, Y. (2012). Study on structural behavior of weldless joint in beam-to-column connection of interior column with knee brace reinforcement. *Stessa 2012 (Behaviour of Steel Structures in Seismic Areas)*, 263-268.

Neves, L. F. C. and Gomes, F. C. T. (1996) Semi-Rigid Behaviour of Beam-to-Column Minor-Axis Joints. *Proceedings of IABSE International Colloquium on Semi-Rigid Structural Connections*, 207-216.

ANSYS Inc. (2011) Theory Reference, ANSYS Release 14.0, 2011.